

# The broad orientation dependence of the motion streak aftereffect reveals interactions between form and motion neurons

**Matthew F. Tang**

School of Psychology, The University of Western Australia, Crawley, Western Australia, Australia



**J. Edwin Dickinson**

School of Psychology, The University of Western Australia, Crawley, Western Australia, Australia

**Troy A. W. Visser**

School of Psychology, The University of Western Australia, Crawley, Western Australia, Australia

**David R. Badcock**

School of Psychology, The University of Western Australia, Crawley, Western Australia, Australia

The extended integration time of visual neurons can lead to the production of the neural equivalent of an orientation cue along the axis of motion in response to fast-moving objects. The dominant model argues that these motion streaks resolve the inherent directional uncertainty arising from the small size of receptive fields in V1, by combining spatial orientation with motion signals in V1. This model was tested in humans using visual aftereffects, in which adapting to a static grating causes the perceived direction of a subsequently presented motion stimulus to be tilted away from the adapting orientation. We found that a much broader range of orientations produced aftereffects than predicted by the current model, suggesting that these orientation cues influence motion perception at a later stage than V1. We also found that varying the spatial frequency of the adaptor changed the aftereffect from repulsive to attractive for motion-test but not form-test stimuli. Finally, manipulations of V1 excitability, using transcranial stimulation, reduced the aftereffect, suggesting that the orientation cue is dependent on V1. These results can be accounted for if the orientation information from the motion streak, gathered in V1, enters the motion system at a later stage of motion processing, most likely V5. A computational model of motion direction is presented incorporating gain modifications of broadly tuned motion-selective neurons by narrowly tuned orientation-selective cells in V1, which successfully accounts for the extant data. These results reinforce the suggestion that orientation places strong constraints on motion processing but in a previously undescribed manner.

## Introduction

How neurons in V1 signal the direction of object motion has been a dominant question in visual neuroscience. An aperture problem arises as the small receptive fields of V1 neurons make elongated contours produce ambiguous motion direction estimates (Adelson & Movshon, 1982). Although pooling multiple signals in higher visual areas can solve this problem (Adelson & Bergen, 1985; Amano, Edwards, Badcock, & Nishida, 2009a), an alternative solution uses the extended integration time of V1 neurons, which causes fast-moving objects to create the neural equivalent response of a spatially extended form cue along the axis of motion (Badcock & Dickinson, 2009; Geisler, 1999; Geisler, Albrecht, Crane, & Stern, 2001). Geisler suggested that multiplicatively combining these motion streaks with motion signals, in V1, gives motion the directional precision of form information. Consistent with this suggestion, presenting a rapid succession of locally uncorrelated patterns with a consistent global pattern results in perception of motion in the global pattern direction (Ross, Badcock, & Hayes, 2000). In addition, motion streaks have been shown to increase sensitivity to global motion and influence perceived motion direction (Apthorp et al., 2013; Burr & Ross, 2002; Edwards & Crane, 2007). There has been evidence showing that fast translational motion leaves an orientation cue (a motion streak) parallel to the motion axis (Apthorp & Alais, 2009; Apthorp, Cass, &

Citation: Tang, M. F., Dickinson, J. E., Visser, T. A. W., & Badcock, D. R. (2015). The broad orientation dependence of the motion streak aftereffect reveals interactions between form and motion neurons. *Journal of Vision*, 15(13):4, 1–18, doi:10.1167/15.13.4.

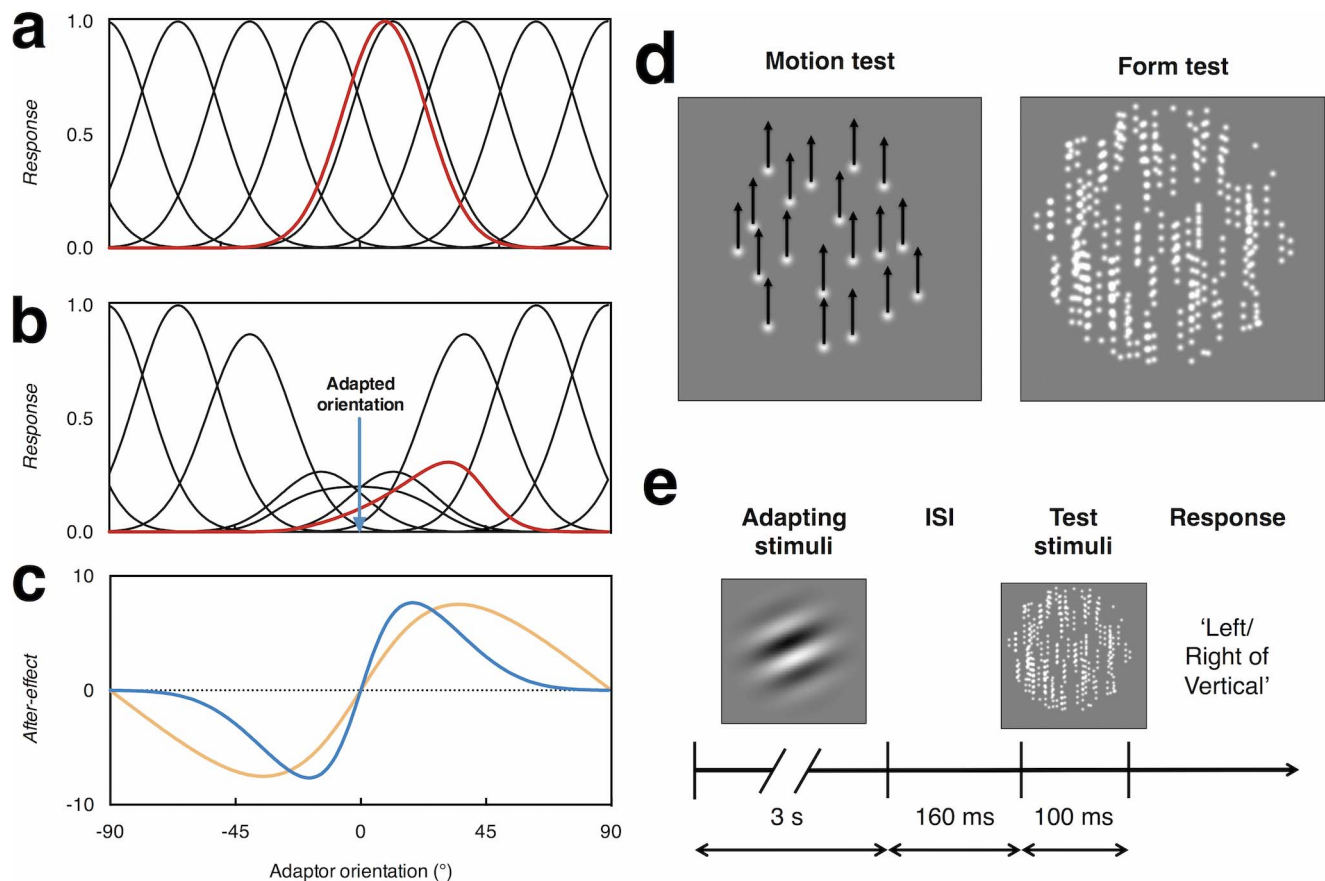
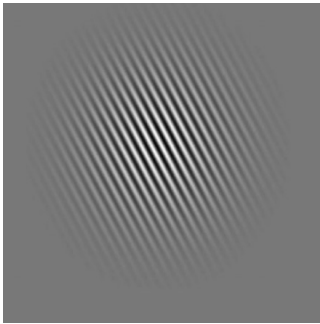


Figure 1. (a–c) A hypothetical example showing how changing neuronal response can account for the TAE using a channel-based model of orientation coding. This example also shows why measuring the angular dependency of the aftereffect estimates the underlying bandwidth of the neuronal population. (a) The seven orientation channels are equally responsive before adaptation to their preferred orientations. The population response is centered at  $10^\circ$  when a stimulus with a  $10^\circ$  orientation is presented prior to adaptation (red curve). (b) The channels selective for the adapted orientation ( $0^\circ$ ) are maximally depressed following adaptation at this orientation. When a stimulus with a  $10^\circ$  orientation is again presented following adaptation, the combined population response shifts away from the veridical orientation. (c) The magnitude of the aftereffect depends on the relationship between the test stimuli's orientation and bandwidth of the adapted neurons. The blue line indicates the predicted aftereffect for the indicated adaptor orientations with narrowly tuned neurons, whereas the yellow line indicates the aftereffects with broadly tuned neurons. (d) Simplified versions of the stimuli used in the motion and form test conditions in the experiment. The arrows indicate the direction of travel for each dot across the four stimulus frames for the motion stimuli. (e) A schematic representation of the trial.

Alais, 2010, 2011; Athorp et al., 2013; Athorp, Wenderoth, & Alais, 2009; Geisler et al., 2001), but a critical test about how this streak is combined with motion direction information has yet to be reported.

Visual aftereffects have been used for many years to noninvasively estimate system properties underlying human perception. The tuning of the orientation mechanisms in V1 has been shown using the tilt aftereffect (TAE; Clifford, 2002, 2014), where adapting to static features causes the perceived orientation of subsequently presented features to be tilted away from the adapted orientation. This effect is dependent on the orientation difference between adaptor and test, with the magnitude of repulsion peaking for separations of  $15^\circ$  to  $20^\circ$ , then declining at larger separations and finally yielding a small attractive aftereffect at separa-

tions near  $75^\circ$  (Clifford, 2002; Gibson & Radner, 1937; Wenderoth & Johnstone, 1988). This roughly corresponds with neurophysiological evidence showing that the response of orientation-selective neurons is biased away from the adapted orientation for nearby but not distant orientations (Figure 1a through c; Dragoi, Sharma, & Sur, 2000) and supports the angular dependence of the TAE being consistent with the orientation bandwidth of V1 neurons (full width at half maximum [FWHM]  $40^\circ$ ; K. K. De Valois, 1977). Notably, however, the angular dependence of motion-direction aftereffects peaks between  $30^\circ$  and  $40^\circ$  (Schrater & Simoncelli, 1998), consistent with the bandwidth of motion-sensitive neurons in V5 (FWHM  $\sim 90^\circ$ ; Albright, 1984; Snowden, Treue, & Andersen, 1992), but not the  $180^\circ$  bandwidth of motion-sensitive



Movie 1. The motion streak aftereffect; the perceived direction of vertical global dot motion appears repelled away from the orientation ( $30^\circ$ ) of the static adapting Gabor.

neurons in V1 (Movshon, Adelson, Gizzi, & Newsome, 1985).

We examined the motion-streak mechanism using a static adaptor to change the perceived direction of motion or orientation of static form stimuli (Movie 1). The angular dependence of the motion direction aftereffect was twice as broad as form and differently modulated by adaptor spatial frequency, suggesting the orientation and motion signals are combined at a later stage of motion pooling, not V1. Using transcranial direct current stimulation (tDCS) to increase the excitability of V1 reduced the aftereffect, suggesting orientation information is inherited from this area. A new model for motion direction is provided in which narrowly tuned orientation-selective neurons modulate broadly tuned motion-selective neurons at a different processing stage.

## Methods

### Observers

Four observers (three men) between 22 and 49 years of age (median = 25 years) took part in all experiments. Authors M. F. T. and J. E. D. participated, whereas the other observers were naïve to the experimental aims. These observers were extensively tested, the data presented here required 89,600 trials, taking approximately 100 hr to collect. The extensive testing and fully within-subjects design, with each acting to replicate the effects, allowed us to be very certain of each observer's performance. There was very little variation reported between the different observers. All observers had normal or corrected-to-normal visual acuity, as measured using a LogMAR chart. The procedure was in accordance with the Declaration of Helsinki and approved by the Human Research Ethics Committee at the University of Western Australia, with all observers providing written, informed consent.

### Apparatus

The stimuli were generated in MATLAB 7.14 on a MacBook Pro (i7, 2.53 GHz) with a NVIDIA GT330M graphics card using PsychToolbox. The stimuli were displayed on a Sony Trinitron G520 monitor with a 120-Hz refresh rate at a resolution of  $1024 \times 786$  pixels using a Cambridge Research System Bits# system to achieve 14-bit grayscale resolution. Observers viewed the monitor from 70 cm (maintained with chin rest), resulting in the display subtending  $31^\circ \times 23^\circ$  (pixel subtense of  $1.8' \times 1.8'$ ). The luminance was gamma-corrected using a Cambridge Research System ColorCAL II and custom-written software. The background display luminance was  $80 \text{ cd/m}^2$ , with a maximum of  $160 \text{ cd/m}^2$ .

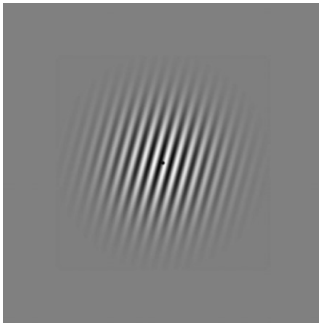
### Stimulus and psychophysical procedure

#### Test stimulus

Global dot motion was used as the motion stimulus, with all 100 dots having Gaussian luminance profiles and translating coherently (Movie 1). The maximum luminance of a dot was  $160 \text{ cd/m}^2$ , and the minimum was  $80 \text{ cd/m}^2$ . The diameter of the dots was  $0.33^\circ$ , equating to four times the standard deviation of the Gaussian luminance distribution. Each dot was randomly positioned within a  $10^\circ$  circular aperture at the beginning of each trial. All dots then translated at  $10^\circ/\text{s}$ , for four stimulus frames (unless otherwise noted), with each frame presented for three refreshes of the monitor (an effective animation rate of 40 Hz), in a consistent global direction. A dot wrapped around the aperture, reappearing on the opposite side, if it was going to move outside the aperture on the next frame. A number of control conditions (described below) were run to evaluate the influence of low-level image properties. The stimuli in the form conditions (Movie 2) were the same as the motion stimuli, but the dots in the four frames were added all to the same frame and presented simultaneously, giving the impression of at least 100 oriented lines (depending on the wrapping).

#### Procedure

Each trial began with a central fixation dot (Figure 1e). An oriented adapting Gabor (a sinusoidal grating modulated by a two-dimensional [2D] Gaussian window) with an envelope standard deviation of  $1.66^\circ$  was then presented. The spatial frequency of the adapting Gabor was  $3 \text{ c}^\circ$ , unless otherwise noted. On each trial, an adaptor was presented for 3 s followed by a 160-ms interstimulus interval before the 100-ms test stimulus was presented (Figure 1c). Observers then indicated whether the test stimulus's direction or orientation was



Movie 2. The static tilt aftereffect, which was used for the form-test condition. Similar to Movie 1, the perceived orientation of the field of lines appears tilted away from the orientation ( $15^\circ$ ) of the adapting Gabor.

to the left or right of vertical using a keyboard. Stimuli were centered  $9^\circ$  to the right of fixation as peripheral presentation increases the magnitude of the aftereffect without affecting its reported angular dependence (Dickinson, Harman, Tan, Almeida, & Badcock, 2012; Muir & Over, 1970), suggesting that there is no effect on angular dependence for using peripheral presentation.

The aftereffect was estimated by measuring the magnitude of direction or orientation repulsion from vertical (depending on the condition) after adapting to an oriented Gabor. The aftereffect's orientation dependence was estimated by varying the orientation of the adapting Gabor ( $-90^\circ$ ,  $-70^\circ$ ,  $-50^\circ$ ,  $-30^\circ$ ,  $-20^\circ$ ,  $0^\circ$ ,  $20^\circ$ ,  $40^\circ$ ,  $60^\circ$ ,  $80^\circ$ ) from vertical in separate blocks of trials. The method of constant stimuli was used to vary the true direction or orientation of the test stimulus with 40 trials presented for each of the seven directions in a pseudo-randomized manner. The order of adapting orientations tested was also pseudo-randomized between the observers. The range of angular deviations of the motion direction or form orientation used for the method of constant stimuli steps was adapted for each observer to measure their entire psychometric function.

## Data analysis

The probability of the observer reporting that the test stimulus orientation or direction was to the right of vertical was calculated for each stimulus direction or orientation. Cumulative Gaussian functions were fitted to these responses in each condition, with the mean indicating the point of subjective equality (i.e., the true direction or orientation the stimuli needs to vary from vertical to be perceived vertical after adaptation). The points of subjective equality for all adaptor orientations were fitted using the first derivative of a Gaussian (D1,

Equation 1), to measure the angular dependence of the aftereffects. All fitting was done using nonlinear regression in GraphPad Prism (6.0c for Mac, Graph-Pad Software, La Jolla, CA), which gives parameter estimates and associated 95% confidence intervals based on the precision of the model fit.

$$D1 = A \times \frac{1}{\sigma} \times \theta \times \exp\left(-\frac{\theta^2}{2\sigma^2}\right) + C \quad (1)$$

$A$  is a free parameter representing the amplitude of the curve.  $\sigma$  is a free parameter representing the width of the function.  $\theta$  is the physical orientation of the adapting Gabor.  $C$  is also a free parameter for a constant offset to correct for any systematic response biases.

## tDCS procedure

Transcranial stimulation was delivered using a constant-current battery-driven stimulator (Dupel Iontophoresis System, St. Paul, MN) through two  $6 \times 4$ -cm saline-soaked electrodes placed in pouches on the scalp. The active electrode was placed directly above the mastoid bone, whereas the reference was placed at position Cz in the International 10-20 System (Homan, Herman, & Purdy, 1987). Both electrodes were aligned along the midline. This montage has previously been shown to increase excitability of the visual cortex with anodal stimulation and decrease excitability with cathodal stimulation, as measured by changes in the early visual component N70 visual evoked potential (Accornero, Li Voti, La Riccia, & Gregori, 2007). The polarity of the electrode placed above the mastoid bone defines the type of stimulation. The current was gradually increased over 30 s to 2 mA at the start of the session and then maintained at this level until the end of testing, where it was decreased to 0 mA over 30 s. Psychophysical procedures began 30 to 60 s after the start of stimulation. Previous work suggests there is no difference in sensation between anodal and cathodal stimulation, meaning that observers were effectively blind to the condition (Tadini et al., 2011). The authors were also blind to stimulation condition until completion of testing as another experimenter conducted the experiment.

## Results and discussion

### The motion streak aftereffect shows broader angular dependence than the TAE

We began by measuring the angular dependence of the motion streak mechanism by examining how the

orientation of an adapting static grating alters the perceived direction of subsequently presented motion. This was compared with the conventional TAE measured using static adaptors and test stimuli. Geisler (1999) showed that adapting to a static orientation repels the perceived direction of subsequently presented motion. He did not, however, measure the angular dependence of this aftereffect nor compare it to the TAE and thus could not determine whether this mechanism has the properties of a narrowly tuned form (which Geisler's model predicts) or a broadly tuned motion system. To address this question, the angular dependence for motion streak test stimuli was compared with that for static versions of the test stimuli in order to compare the tuning of the motion streak mechanism to that of the static-form angular dependence.

Figure 2 shows the magnitude of the aftereffect plotted against the adaptor orientation. The normal TAE was obtained in the form-test condition with the perceived orientation of the stimuli repelled away from the adaptor, with maximum repulsion occurring when the adaptor was oriented about 20° from vertical (Clifford, 2002; Clifford, Wenderoth, & Spehar, 2000; Dickinson, Almeida, Bell, & Badcock, 2010; Dickinson et al., 2012; Gibson & Radner, 1937; O'Toole & Wenderoth, 1977). The perceived motion direction was repelled away from the direction of the adapting orientation in the motion-test condition, showing the static-induced direction aftereffect (SI-DAE). The maximum direction repulsion, however, occurred when the adaptor was about 40° from vertical, which is similar to the angular dependence previously reported in the direction aftereffect (Kohn & Movshon, 2004; Levinson & Sekuler, 1976; Schrater & Simoncelli, 1998) and double that found in the same observers in the form-only condition.

D1 functions (Equation 1) fitted to each observer's data yield a  $\sigma$  value that estimates the angular dependence of the aftereffect. A paired-samples  $t$  test comparing  $\sigma$  for the motion- and form-test conditions shows the motion-test condition was broader than in the form-test condition,  $t(3) = 8.04$ ,  $p = 0.004$ ,  $R^2 = 0.96$ . This suggests that the presence of a motion streak does not cause motion to be processed entirely by the same set of orientation-tuned mechanisms as form stimuli, as predicted by Geisler (1999). The model would predict a narrower range of orientations causing aftereffects, and the results suggest that orientation is affecting only perceived motion direction at a later stage of the processing hierarchy. The angular dependence is consistent with the direction aftereffect and the broad bandwidths of motion-selective neurons in V5 (Albright, 1984; Britten & Newsome, 1998; Rodman & Albright, 1987; Snowden et al., 1992) as a full-width at half-height bandwidth measurement of 90°, which is

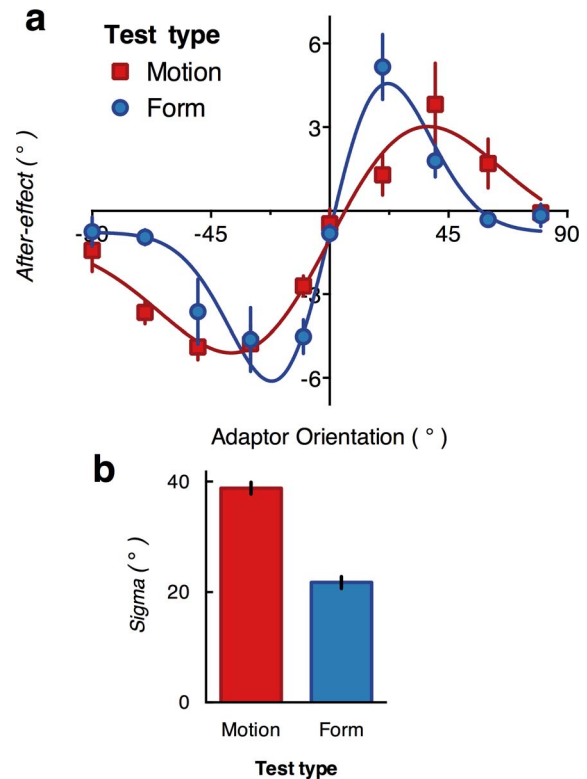


Figure 2. (a) The magnitude of the aftereffect measured using motion (SI-DAE) and static (TAE) dot test stimuli following adaptation to static Gabors of various orientations ( $n = 4$ ). A positive value of the adaptor orientation indicates the grating is rotated anticlockwise from vertical, whereas positive indicates clockwise rotation. The fitted function is a first derivative of a Gaussian (D1). The error bars represent  $\pm 1$  standard error. (b) The average angular dependence (sigma values of the fitted D1 function) across observers for the fitted D1 curves for the two conditions. The error bars represent within-subjects  $\pm 1$  standard error.

often reported for MT neurons, is equivalent to a 40° width of the Gaussian-derivative function we fitted to the data (mean  $\sigma = 38.82$ , 95% confidence interval [CI] = 35.43–42.20).

## Controlling for low-level image properties

We will now report a number of control experiments that showed that the broader angular dependence for the motion stimulus was due to properties of mechanism tuning rather than the low-level properties of the stimuli. In the first two control conditions (half form and half motion), we increased the range of orientation content of the test stimuli by 50% (Figure 3c to e). See Figure 3 for a detailed explanation. These conditions were the same as the previous task, but only two frames were presented, yielding shorter, less precisely oriented form or motion signals. The behaviorally measured

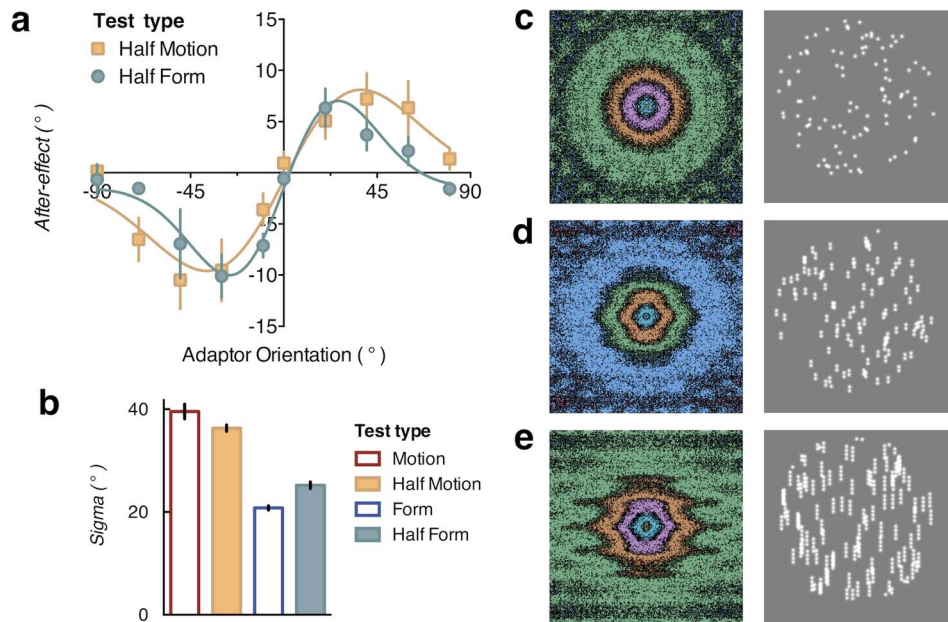


Figure 3. (a) The magnitude of the aftereffects plotted against the adaptor orientations in the control conditions with the half form (TAE) and half motion (SI-DAE) stimulus ( $n = 3$ ). The error bars indicate  $\pm 1$  standard error. (b) The mean sigma values of the fitted D1 functions for these conditions compared with the sigma values in the original experiment. The error bars represent within-subjects  $\pm 1$  standard error. (c–e) Gaussian-dots stimuli with dot repetitions of one (c), two (d), or four (e), plotting the two-dimensional Fourier spectrum in the left column and a corresponding example of the stimulus in the right. The frequency response for the stimuli was taken from the average Fourier spectrum of 2,500 iterations of each stimulus type (to control for the randomization of each stimulus in the experiment). The orientation spectrum becomes elongated as more dots are added to the line segments, showing that the energy in the orientation spectrum is more concentrated in the direction of elongation in the full- compared with half-form condition. This was confirmed when we took the full-width at half-height measurements for response to vertical orientation across conditions. The full-form condition ( $10.35^\circ$ ) had a much narrower orientation spectrum than the half-form condition ( $15.35^\circ$ ).

angular dependence for the half-form condition was similar to the full-form condition; likewise, angular dependence did not vary between the half- and full-motion conditions (Figure 3). A paired-samples  $t$  test failed to find a difference in  $\sigma$  between the full- (mean  $\sigma = 39.59$ , 95% CI = 33.34–45.78) and half-motion (mean  $\sigma = 36.32$ , 95% CI = 33.64–38.99) condition,  $t(2) = 1.63$ ,  $p = 0.25$ ,  $R^2 = 0.57$ . Likewise, the tuning function of the full- (mean  $\sigma = 20.80$ , 95% CI = 18.98–22.61) and half-form (mean  $\sigma = 25.23$ , 95% CI = 22.46–27.99) conditions was similar although statistically significantly different,  $t(2) = 9.59$ ,  $p = 0.01$ ,  $R^2 = 0.98$ . This shows that under these conditions, these functions are not limited by the intrinsic orientation uncertainty in the stimulus as smearing the orientation information over a broader range in the half-motion and -form conditions did not alter the angular dependence of the aftereffects by equivalent amounts. This suggests that the orientation uncertainty in the stimuli was less than that in the mechanisms detecting the orientation/direction, meaning that the measured angular dependence is not caused by stimulus-specific parameters.

A further control condition examined whether the spatial frequency profile of the test stimuli affected the measured angular dependence of the SI-DAE. This

experiment was motivated by the finding that orientation selectivity of V1 neurons in macaque becomes increasingly broad with higher spatial frequency stimuli (R. L. De Valois, Albrecht, & Thorell, 1982). The spatial frequency content of the stimuli may explain the different orientation dependencies of the form and motion-test stimuli because the dots had a Gaussian profile with a small sigma and therefore a broad spatial frequency profile (Figure 4a to c). To test this option, we measured the angular dependence of the SI-DAE using dots with a luminance profile of a fourth derivative of a Gaussian (D4), which changed the peak spatial frequency from  $0\text{ c}/^\circ$  to  $7.3\text{ c}/^\circ$ . We also changed the spatial frequency of the adaptor to  $7.3\text{ c}/^\circ$  to coincide with the spatial frequency of the dots. Results obtained with this modified procedure were similar to the initial experiment. A paired-samples  $t$  test showed the  $\sigma$  values between the Gaussian- and D4 test-motion conditions were not significantly different,  $t(2) = 1.47$ ,  $p = 0.28$ ,  $R^2 = 0.51$ . Taken together, these control experiments demonstrate that the angular dependence of the SI-DAE was not due to these stimulus-specific attributes and, instead, suggests the results reflect mechanism tuning.

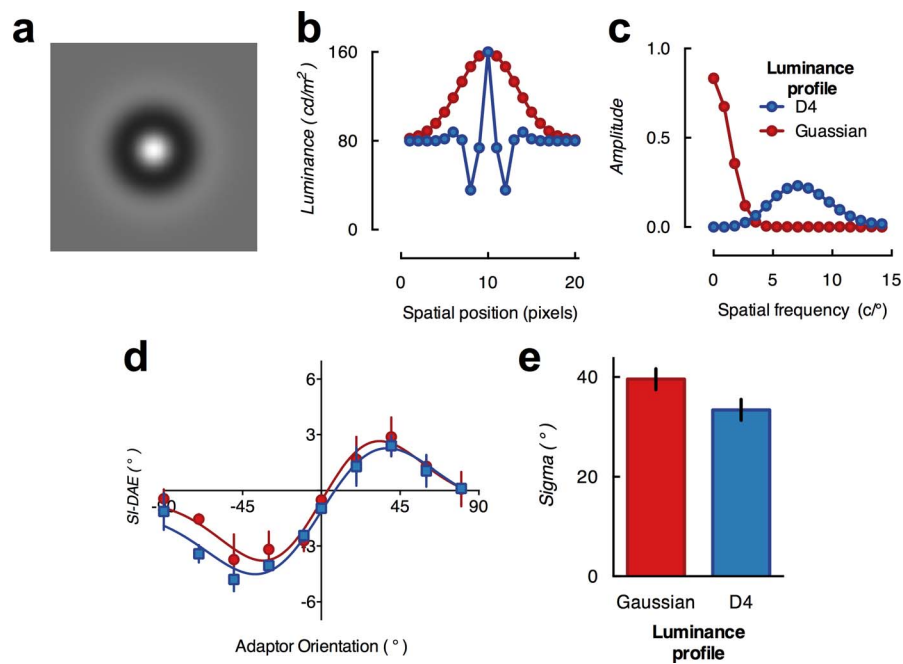


Figure 4. (a) An enlarged version of the dots used in the D4 condition. (b) The luminance profile of a horizontal slice through the middle of the D4 dot compared with the normal Gaussian dot. (c) The spatial frequency profile of the D4 dot, the peak spatial frequency occurred at  $7.5\text{ c}/^\circ$ , compared with the Gaussian dot, the peak spatial frequency occurs at  $0\text{ c}/^\circ$ . (d) The magnitude of the aftereffect for the D4 (blue line) and Gaussian (red line) dots plotted against the orientation of the adaptor ( $n = 2$ ). The error bars indicate  $\pm 1$  standard error. (e) A summary graph of the sigma values of the fitted functions for the observers. The error bars represent within-subjects  $\pm 1$  standard error.

## Orientation and motion-selective neurons have a reciprocal relationship

In a previous study, Apthorp and Alais (2009) argued that adapting to streak-inducing motion leads to a TAE with similar angular dependence to the standard TAE. Importantly, however, they drew this conclusion by comparing their results to previous reports of the TAE gathered from different subjects using different stimuli. To ensure direct comparability, we used a within-subjects design to reexamine the impact of streak-induced motion on the TAE. To do this, we reversed the stimulus types from the first experiment with observers adapting to 3 s of fast-moving translational motion that varied in direction followed by a test static Gabor stimulus that was oriented around vertical. The direction of the adapting motion was varied across blocks to sample the entire direction-orientation function.

Adapting to oriented motion direction caused a small change in the perceived orientation of the static-test Gabor away from the adaptor direction (Figure 5). The magnitude of this aftereffect was slightly smaller than that reported by Apthorp and Alais (2009). This is likely due to the shorter adaptation time used in the current study, which has an inverse exponential relationship with the magnitude of the aftereffect

(Greenlee & Magnussen, 1987; Magnussen & Johnsen, 1986). The smaller magnitude of the aftereffects, however, should have little effect on the measured angular dependence (Dickinson et al., 2012).

The angular dependence was broader than for the form-adapt and form-test condition but slightly narrower for the SI-DAE measured in the previous experiments. As the angular dependence of this aftereffect was somewhere between the motion-test and form-test condition, it suggests that the motion streaks are adapting narrowly tuned orientation-selective neurons in addition to the broad influence of motion neurons exerting gain on orientation. In the modeling section, we show that the angular dependence in this condition can be accounted for by broadly tuned motion-selective neurons modulating the gain of narrowly tuned orientation-selective neurons, with the presence of the motion streak also causing additional adaptation of orientation-selective neurons. This result suggests motion-selective neurons in V5 may reciprocally influence orientation-selective neurons in V1.

These results also rule out a possibility that the form and motion test stimuli after adapting to static form are activating different populations of V1 neurons. It is possible that the motion-test stimuli activate neurons perpendicular to the motion axis and neurons parallel to the motion axis because of the motion streak. The form-test stimulus, however, may be activating neurons

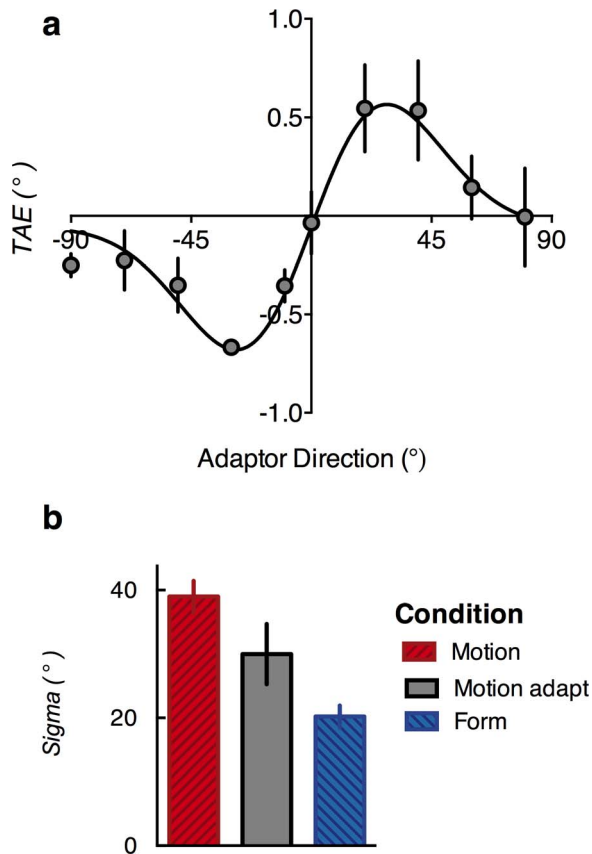


Figure 5. The effects of adapting to motion on the perceived orientation of subsequently presented static Gabors. (a) The magnitude of the TAE plotted against the direction of the adapting motion direction ( $n = 4$ ). The error bars indicate  $\pm 1$  standard error. (b) A summary graph of the sigma values of the fitted functions for the observers. The error bars indicate within-subject  $\pm 1$  standard error.

only parallel to the orientation, as the test stimulus does not move. It is therefore possible that motion-test stimuli are activating a broader range of neurons than activated by the form-test stimuli. However, the results for the motion-adapt condition suggest this is not the case. If the motion stimuli were activating both parallel and perpendicularly oriented neurons, the D1 function would be a poor fit to the aftereffects, as sizable aftereffects would emerge at very large adaptor directions ( $\pm 75^\circ$ – $90^\circ$ ). Contrary to this prediction, this function provided a very good fit to the data (mean  $R^2 = 0.84$ ,  $SD = 0.04$ ).

### Spatial frequency selectivity of SI-DAE

The static TAE is selective for spatial frequency, with the greatest aftereffect occurring when both test and adaptor stimuli have the same spatial frequency and decreasing as the difference in spatial frequency of adaptor and test increases. The aftereffect disappears

when there is more than one octave difference in spatial frequency between the adaptor and test (Ware & Mitchell, 1974). These behavioral findings are consistent with neurophysiological measurements of spatial frequency selectivity of neurons in V1 (R. L. De Valois, William Yund, & Hepler, 1982). On the other hand, global motion integrates across spatial frequency, consistent with the neurophysiological findings that V5 neurons are broadly tuned for spatial frequency (Amano, Edwards, Badcock, & Nishida, 2009b; Bex & Dakin, 2002; Movshon & Newsome, 1996; Simoncelli & Heeger, 1998). The broad angular dependence of the motion streak aftereffect suggests the aftereffect is dependent on the stage of global motion pooling, most likely at V5. On this logic, the SI-DAE would be predicted to show a different spatial frequency dependency compared with the static TAE. To test this prediction, we examined the effect of varying the spatial frequency of the adaptor on the magnitude of the SI-DAE and TAE. The same procedures were used as in the first experiment but with the magnitude of the aftereffect measured with one adaptor orientation ( $20^\circ$ ), which varied in spatial frequency.

We replicated the spatial-frequency specificity of the TAE in the form condition with the aftereffect being largest when the adaptor was 1 to 4  $c/^\circ$  and reduced when the adaptor had a lower or higher spatial frequency than this, finally disappearing at higher spatial frequencies (Figure 6). The effective spatial frequency of the form dots may have resulted in this spatial frequency tuning because of the observer's contrast sensitivity for a Gaussian dot. This can be given by multiplying the typical contrast sensitivity at 10 Hz (Robson, 1966), the presentation rate of the test, with the spatial frequency spectrum of the Gaussian dot (Figure 4c). This manipulation means the function peaks at 0 to 4  $c/^\circ$  before reducing to zero at the higher spatial frequencies. A masking study found similar spatial frequency tuning for streak-inducing Gaussian dots with similar properties (Apthorp et al., 2011).

Most importantly and surprisingly, in the motion condition, the SI-DAE went from repulsive to attractive when the spatial frequency of the adaptor was changed. We believe this arises because of the increased contrast sensitivity that occurs when the adaptor and test are separated by more than two octaves of spatial frequency (K. K. De Valois, 1977). This explanation is consistent with the orientation information from the motion streak first affecting the perceived motion direction at the level of global motion processing, most likely V5, which receives inputs from a broad range of spatial frequencies, rather than V1, which is selective for a narrow range of spatial frequencies (Movshon & Newsome, 1996).

This attractive effect can be explained if it is assumed that sensitivity is decreased by adaptation for nearby

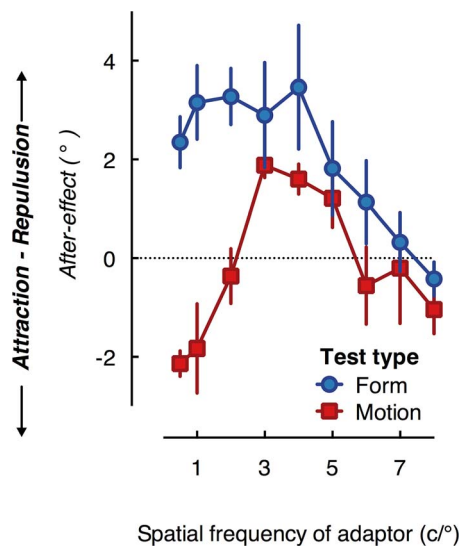


Figure 6. The magnitude of the motion- (SI-DAE) and form-test (TAE) following adaptation to a Gabor with a  $20^\circ$  orientation ( $n = 4$ ) as a function of spatial frequency. Response bias was removed from each observer's results by the constant offset value measured in the first experiment. Error bars indicate  $\pm 1$  standard error.

spatial frequencies but increased when there are more than two octaves of difference following adaptation (Blakemore & Campbell, 1969; K. K. De Valois, 1977; Greenlee & Magnussen, 1988). Interactions between neighboring V1 neurons with different spatial frequencies are thought to cause spatial frequency-dependent changes (both excitatory and inhibitory) of contrast sensitivity with adaptation (K. K. De Valois, 1977). Changing from inhibitory response at the same spatial frequency to an excitatory response at different spatial frequencies can thus explain the change from repulsive to attractive aftereffects.

This attractive aftereffect is particularly interesting because in the TAE, perceived orientation is not attracted following adaptation to gratings with different spatial frequencies (Carandini & Ferster, 1997; Dickinson & Badcock, 2013; Ware & Mitchell, 1974). Perceived orientation can, however, exhibit spatial frequency-dependent attraction and repulsion during simultaneous, rather than sequential, presentation, which can be accounted for by the same change from inhibitory to excitatory gain modulation (Dickinson et al., 2012; Skillen, Whitaker, Popple, & McGraw, 2002). The difference between the SI-DAE and the TAE may be due to the broad spatial frequency tuning of V5, as the inputs from separate spatial frequencies would influence the same motion representation (Bex & Dakin, 2002; Movshon & Newsome, 1996; Simoncelli & Heeger, 1998), compared with the narrow spatial frequency tuning in V1 (R. L. De Valois, William Yund, & Hepler, 1982),

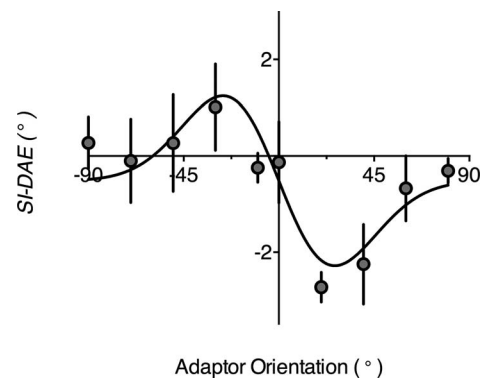


Figure 7. The magnitude of the SI-DAE as a function of the orientation of an adapting  $1\text{ c/}^\circ$  Gabor ( $n = 3$ ), showing an attractive aftereffect. Error bars indicate  $\pm 1$  standard error.

where the TAE is generally thought to arise (Fang, Murray, Kersten, & He, 2005).

The unexpected change from a repulsive to attractive aftereffect motivated us to measure the full orientation function for the attractive SI-DAE to further investigate its origins. To do this, the same procedure was used as in the first experiment, but the spatial frequency of the adaptor was changed from  $3\text{ c/}^\circ$  to  $1\text{ c/}^\circ$ , as adapting to a  $1\text{ c/}^\circ$  static Gabor caused a large attractive aftereffect in the previous experiment. The attractive effect occurs for all tested adaptor orientations, with the magnitude of the effect peaking when the adaptor orientation was  $\sim 35^\circ$  from vertical (Figure 7). This is similar to the width of the function we found in the first experiment for a repulsive aftereffect with a  $3\text{ c/}^\circ$  adaptor, suggesting they may be represented in the same set of broadly tuned neurons. As our attractive aftereffects are well described by the first derivative of a Gaussian (D1) function, it is reasonable to suggest that the same channel-based mechanism could be responsible for both the attractive and repulsive effects, as we will show in our model below.

### Increasing excitability of V1 reduces the magnitude of the SI-DAE

The results from the previous experiments strongly suggest the orientation information from motion streaks influences motion direction processing at the stage of global motion pooling, most likely V5. This is contrary to the currently dominant model that argues solely for the involvement of V1. To further investigate the involvement of V1 in our effects, we used tDCS, a noninvasive brain stimulation technique, to alter cortical excitability. Anodal tDCS increases and cathodal tDCS decreases excitability by altering the resting membrane potential of the stimulated neurons (Nitsche et al., 2003; Stagg & Nitsche, 2011), as shown

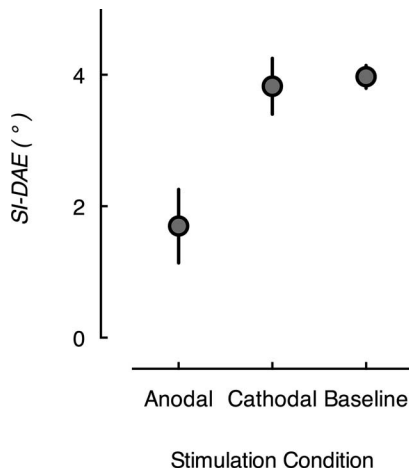


Figure 8. The group magnitude of the SI-DAE during anodal and cathodal tDCS stimulation compared with baseline performance ( $n = 4$ ). The error bars indicate within-subject  $\pm 1$  standard error.

by concomitant changes in corticospinal excitability (Nitsche et al., 2003; Nitsche & Paulus, 2000) and hemodynamic response (Lang, Nitsche, Paulus, Rothwell, & Lemon, 2004).

Stimulation over the occipital pole alters early components of the visual evoked potential (Accornero et al., 2007) and shows polarity-dependent modulation of V1 excitability (Antal, Kincses, Nitsche, & Paulus, 2003). The effect of tDCS applied over the visual cortex appears to be relatively specific to the location of stimulation, with neuroimaging showing that stimulating V5 increases excitability in this area but not V1 (Antal et al., 2012). This is mirrored by behavioral results with learning on a motion task improved when stimulation was delivered to V5 but not when delivered to V1 (Antal, Nitsche, et al., 2004), and the duration of motion aftereffects is reduced only when stimulation is delivered over V5 with no corresponding effect when delivered over V1 (Antal, Varga, et al., 2004). It thus appears likely that excitability changes are relatively localized at the targeted stimulation site.

We examined the effect of applying tDCS over V1 on the SI-DAE to determine whether this area is involved in the aftereffect (Figure 8). A one-way repeated-measures analysis of variance revealed significant effects of stimulation condition on the magnitude of the SI-DAE,  $F(2, 11) = 6.22$ ,  $p = 0.034$ ,  $R^2 = 0.67$ . Post hoc comparisons with Bonferroni correction indicated that anodal tDCS reduced the magnitude of the aftereffect compared with the baseline condition (adjusted  $p < 0.05$ ), but there was no difference between the cathodal and baseline conditions (adjusted  $p > 0.05$ ). This result supports previous studies showing that motion streaks are formed in early visual areas (Apthorp & Alais, 2009; Apthorp et al., 2013; Geisler et al., 2001). Adapting to an oriented feature causes orientation-

specific hyperpolarization of neurons in V1 (Carandini & Ferster, 1997), which leads to the TAE through a reduction in contrast sensitivity to nearby orientations (Blakemore & Campbell, 1969; Clifford, 2014). We hypothesize that the reduction of the aftereffect with anodal tDCS may be because increasing the excitability of neurons in V1 reduces the hyperpolarization of the oriented channels during adaptation. This, in turn, suggests that early visual cortical areas are involved in the aftereffect, in addition to later processing stages already identified in our previous experiments.

## An alternative model of motion streak input to motion perception

Geisler's (1999) original model of motion streak processing posited that form information, detected by orientation-selective neurons, is multiplicatively combined with motion-sensitive information in V1. This combination results in direction information having the precision of spatial information (Geisler, 1999; Geisler et al., 2001). Our results, however, suggest that this model needs to be reconsidered because the angular dependence of motion streak aftereffects is similar to that of motion signals measured using test stimuli (gratings and plaids) that would not produce motion streaks (Schrater & Simoncelli, 1998) and double that of the angular dependence for orientation. The spatial frequency dependency of the aftereffect also suggests that orientation is affecting the stage of global motion integration. An alternative model can describe these results using narrowly tuned orientation-selective neurons feeding either inhibitory or excitatory gain to a separate population of more broadly tuned direction-selective neurons at a later stage of the processing hierarchy. Figure 9a, b shows a schematic representation of this proposed model of motion streak processing. Rather than providing a comprehensive account of the visual processing, we hope to show with a simple algorithmic model that orientation can affect motion direction processing, which will account for our observed pattern of results. In this regard, the model is complementary to existing theories of motion processing (i.e., intersection of constraints and vector averaging, which would not predict that adapting to orientation changes motion direction) but allows form information to constrain the overall solution. The model thus illustrates a general principle of form-motion interactions, described at a high level. Later studies could apply these principals to models working on natural image sequences.

The model consists of separate banks of orientation- and motion-selective channels. Orientation is represented in double-angle space, encompassing all  $180^\circ$  of orientation, and motion is represented in single-angle

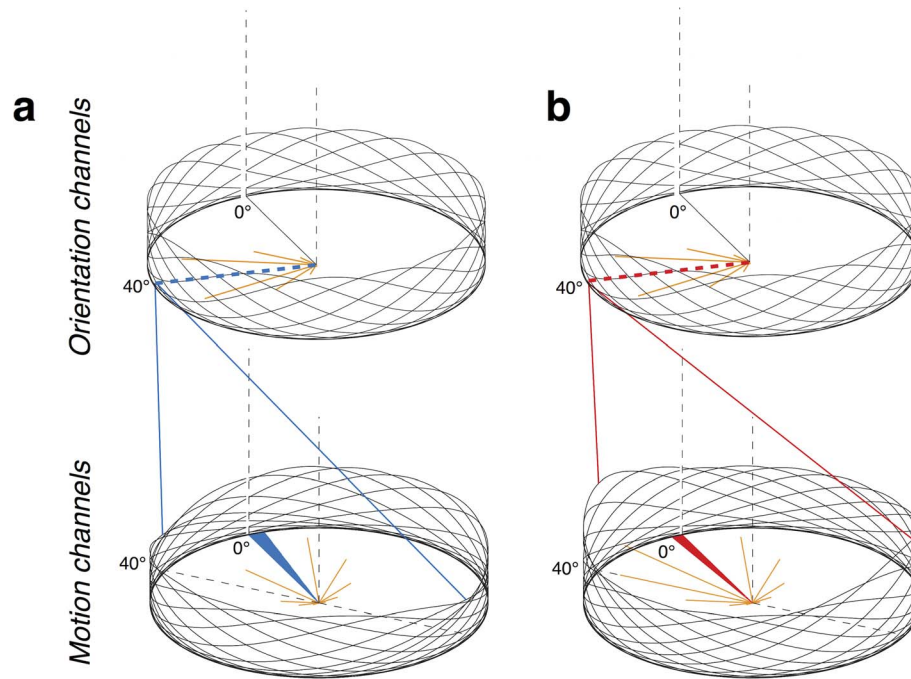


Figure 9. (a–b) A schematic of the model showing how inhibitory (a) or excitatory (b) input from orientation channels to motion channels can cause the observed direction aftereffect. The height of the channel indicates the sensitivity of that channel. The bandwidth parameter of the orientation-selective channels was set to  $15^\circ$  and the motion-sensitive channels were set to  $40^\circ$ . In the examples, a static adapting stimulus is presented with an orientation of  $40^\circ$ , and test at  $0^\circ$ , provides either an inhibitory (a) or excitatory (b) input to the motion channels sensitive to directions of  $40^\circ$  and  $220^\circ$ . The perceived direction of vertical motion is either repelled from (a) or attracted to (b) the adapting orientation. The perceived aftereffect is indicated by the filled in slices of blue (a) or red (b)—note they are on opposite sides of  $0^\circ$ .

space, encompassing all  $360^\circ$  of motion direction (Clifford et al., 2000). Each channel has a Gaussian sensitivity profile that is centered on its preferred orientation or motion direction. The channel's orientation or motion selectivity is evenly spaced to represent double- or single-angle space (Equation 2). The perceived orientation or motion direction is encoded in the collective response of the bank of channels. When a stimulus is presented, it activates a number of channels within the bank that are preferably sensitive to the stimulus parameters. The perceived motion direction is the vector sum of the response of the motion channels to the test stimulus given their sensitivity profiles to the presented motion direction.

$$R(x) = \alpha \times \exp\left(-\frac{(x+c)^2}{2\sigma^2}\right) \quad (2)$$

A variation of a standard Gaussian equation gives the sensitivity profile ( $R$ ) of each orientation and motion-selective channel in the current model.  $\alpha$  represents the amplitude of the Gaussian profile.  $\sigma$  represents the width of the profile that varies to change the channel's bandwidth parameter.  $c$  is used to vary the orientation or motion direction that the channel is centered.

The width of the Gaussian sensitivity profiles representing the orientation-selective channels is set at  $15^\circ$  (equivalent to an FWHM of  $35^\circ$ ), and the direction-selective channels are set at  $40^\circ$  (equivalent to an FWHM of  $94^\circ$ ). Both of these values are consistent with considerable neurophysiological and psychophysical evidence of the average tuning for orientation-selective neurons in V1 and motion direction-selective neurons in V5, respectively (Albright, 1984; Britten & Newsome, 1998; Clifford, 2002, 2014; R. L. De Valois, William Yund, & Hepler, 1982; Gibson & Radner, 1937; Rodman & Albright, 1987; Schrater & Simoncelli, 1998; Snowden et al., 1992). This estimate of the V5 bandwidth is inconsistent with motion-selective neurons in V1 that are responsive to  $180^\circ$  of motion direction for extended contours (Movshon et al., 1985). We chose to base the bandwidth parameters on these locations, as there is very strong evidence that, in humans, adaptation to static gratings cause large changes in V1 (Fang et al., 2005; McDonald, Seymour, Schira, Spehar, & Clifford, 2009; Tootell et al., 1998) and the static orientation cue from the motion streak is detected in this area (Basole, White, & Fitzpatrick, 2003; Geisler et al., 2001). V5 was chosen because this area has been strongly linked to global motion perception in humans (Beckers & Zeki, 1995; Born &

Bradley, 2005; ffytche, Guy, & Zeki, 1996; Morrone, Burr, & Vaina, 1995; Smith, Snowden, & Milne, 1994). Furthermore, V5/MT, unlike V1, contains pattern-selective neurons that are not subject to the aperture problem (Kumano & Uka, 2013; Movshon et al., 1985), with only a small number of the neurons needed to give psychophysical performance on a motion task (Shadlen, Britten, Newsome, & Movshon, 1996).

When an adapting stimulus is presented, the channels that are responsive to that orientation are suppressed (in proportion to their activation to that stimulus, which is given by the Gaussian sensitivity profile for each channel to the orientation of the stimulus). Each orientation-selective channel is linked to the two motion direction-selective channels along the motion axis, due to the change from double- to single-angle space. For example, an orientation-selective channel centered at  $40^\circ$  is linked to two motion-selective channels, one centered at  $40^\circ$  and the other centered at  $220^\circ$ . The orientation-selective channels provide gain (ranging from inhibitory to excitatory) to the motion-selective channels, modifying the sensitivities of the motion-selective channels in proportion to the activity of the corresponding orientation-selective channels during adaptation.

The gain-induced changes in the channel's sensitivity following adaptation are reflected in contrast sensitivity decreasing following adaptation to the same spatial frequency (Blakemore & Campbell, 1969; Ware & Mitchell, 1974) but increasing when the spatial frequency varies by two octaves (K. K. De Valois, 1977). Changing the gain from inhibitory to excitatory reverses the aftereffects from repulsive to attractive (Figure 9a to b), consistent with our empirical findings when the spatial frequency of the adaptor changes by two octaves. The perceived motion direction, given by the population response, is either attracted or repulsed away from the adaptation orientation because, during adaptation, the sensitivity of the bank of channels has been depressed or elevated around the adapting orientation.

To model the results from the form-only condition, the same bank of orientation-selective channels is used for both adaptation and test. This same model has been used to successfully account for both the repulsive TAE and attractive orientation illusions (Dickinson et al., 2012). To model the results in the motion-adaptor condition, adaptation gain from motion-selective channels feeds into the orientation-selective channels. Because the streak will leave the neural equivalent of an oriented form cue along the axis of motion, additional adaptation of the orientation channels aligned with the motion direction was allowed. This stage could be incorporated into the main motion streak model without affecting the results, as the streak is in the direction of the motion

stimulus, meaning there would be no effect on direction. The model's only free parameter is the gain between the banks of channels.

The input to the model is the orientation or motion direction of the adapting and test stimulus consistent with the parameters used when gathering the experimental data. The motion direction input was a direction representing the 2D motion vector. This was used because the true motion direction is the dominant signal with the 100% coherent global dot motion stimulus used in the experiment, which allows observers to discriminate motion direction with very high levels of certainty (Edwards & Badcock, 1994; Webb, Ledgeway, & McGraw, 2007). The proposed gain relationship between orientation and motion neurons outlined here could allow form information to affect different motion-pooling solutions (e.g., intersection of constraints, vector averaging) in a manner that is currently unpredicted.

We used the model to predict the magnitude of the aftereffect following adaptation to the same orientations and directions used in the experiments measuring the angular dependence of the aftereffects (Figure 10). Extra sum-of-squares *F*-tests (Motulsky & Christopoulos, 2004) indicated the model's predictions did not significantly differ from the observed results (all *ps* > 0.05), suggesting that the model provides a good explanation for the extant results.

We can also account for the halving of the SI-DAE when we increased the excitability of V1 using anodal tDCS by reducing gain between orientation- and motion-selective neurons. The model's predictions are also relatively robust to the bandwidth parameters of the motion-selective channels. We examined the effects on the sigma of the resultant D1 function of varying the bandwidth parameter of the motion-selective channels while holding the bandwidth parameter of the orientation-selective channels constant. This showed that after the sigma value of the channels exceeded  $40^\circ$ , the estimated angular dependence of the aftereffect remains relatively constant (Figure 11).

## Conclusions

Our results demonstrate that motion streaks, which arise from the extended integration time of neurons in V1 yielding the neural equivalent of a form cue along the axis of motion, contribute to the perceived direction of motion by a different neural mechanism than is currently thought. The dominant model argues that orientation-selective neurons in V1 detect the streak and that this information is combined in the same stage with motion (Geisler, 1999; Geisler et al., 2001). Our results, instead, suggest that streak-inducing motion

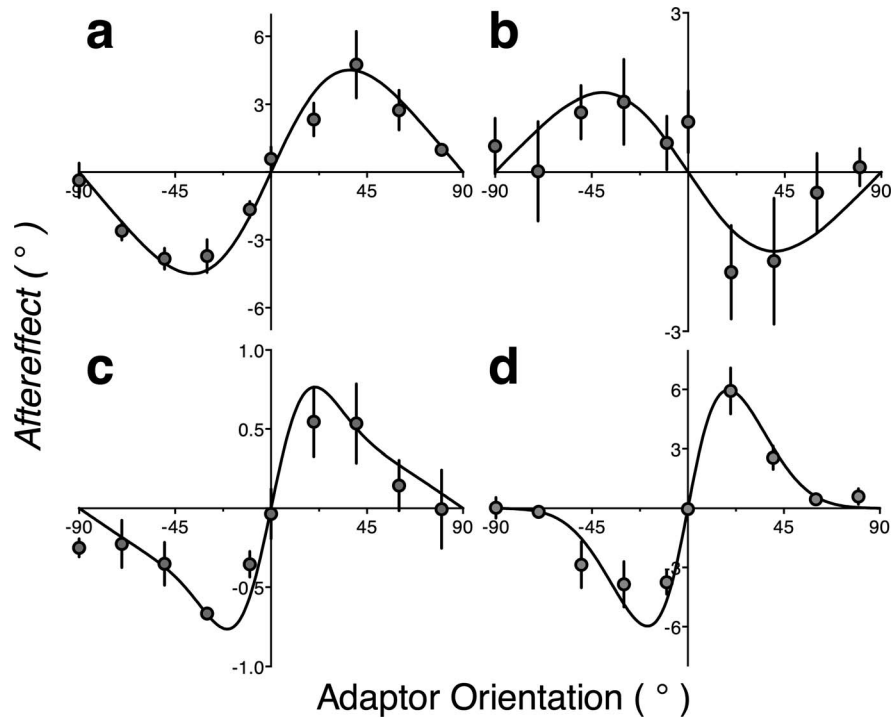


Figure 10. Model predictions (lines) plotted against pooled data across the observers (dots). (a) Angular dependence of the SI-DAE (form-adapt [3 c/°], motion-test). (b) Angular dependence of the attractive SI-DAE (form-adapt [1 c/°], motion-test). (c) Angular dependence of the TAE with a motion-adaptor form-test condition. (d) Angular dependence of the TAE (form-adapt, form-test).

stimuli are detected by narrowly tuned orientation-selective neurons at an early stage, which feed gain into direction-selective neurons at a later stage of motion processing, most likely V5, the stage of global motion integration. This conclusion follows because the aftereffect was reduced when the excitability of V1 was increased using tDCS, suggesting the involvement of V1, and because of the broad tuning and spatial frequency dependency of motion aftereffects, which suggest the involvement of V5.

We created a computational model with narrowly tuned orientation-selective neurons (purportedly in V1) feeding gain into broadly tuned motion-selective neurons (proposed to be in V5) that accurately describes these results. This model is consistent with previous research showing that motion streaks activate orientation-selective neurons in V1 (Apthorp et al., 2013; Basole et al., 2003; Geisler et al., 2001) but adds a unique interaction with motion processing at a higher stage. Unlike most existing theories, we suggest that the streak information gathered at an earlier stage first influences motion direction processing at a later stage of the processing hierarchy. We believe that V5/MT is the later area of processing for a number of reasons. First, neurons in this area are broadly tuned, consistent with the broad angular dependence of the motion streak aftereffect (Albright, 1984; Snowden et al., 1992). Second, intersection-of-constraint-like in-

formation appears to be first integrated in this area from direction-selective input from V1 that is subject to the aperture problem (Heeger, Simoncelli, & Movshon, 1996; Kumano & Uka, 2013; Movshon & Newsome, 1996). It therefore seems possible that orientation information, also gathered in V1, inputs the motion direction computation at this later processing stage in the manner described.

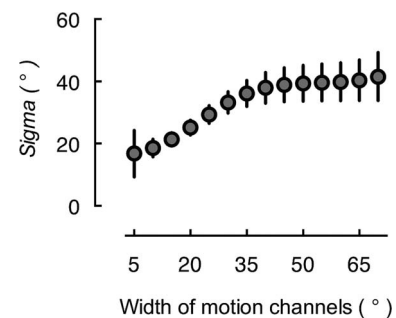


Figure 11. The effects of varying the bandwidth parameter of the motion-selective channels on the width of the angular dependence estimated by fitting the results with the D1. Here we varied the bandwidth parameter of the motion-sensitive channels while holding the bandwidth parameter orientation-selective channels constant at 15°. The error bars represent the 95% confidence intervals associated with the goodness of fit to the stimulated data.

Although clearly not a definitive description of the visual system, we believe that our model provides a significant advance in understanding how form information can constrain motion processing. Indeed, the model can account for a variety of phenomena in the empirical literature. The model is consistent with our recent demonstration that form information enters the motion system by, at least, the stage of global motion pooling (Tang, Dickinson, Visser, Edwards, & Badcock, 2013). The model also explains why the presence of a motion streak enhances contrast sensitivity for both single moving dots (Geisler, 1999) and global motion (Edwards & Crane, 2007). The model predicts that the orientation cues from motion streaks could enhance the motion signal through gain adjustments when they are coincident with the motion direction leading to increased motion direction sensitivity. In addition, the same mechanism described in the model can also explain why providing orientation information at the edge of apertures or adding oriented static lines to the background of a display changes the perceived direction of motion (Badcock, McKendrick, & MaWyatt, 2003; Edwards, Cassanello, Badcock, & Nishida, 2013; Khuu, 2012; Kooi, 1993).

The model also provides a description of why presenting Glass patterns without any consistent motion signal, but with a consistent global pattern, results in the perception of motion in the global pattern direction (Badcock & Dickinson, 2009; Ross, 2004; Ross et al., 2000). Consistent with the model, these patterns activate motion-sensitive areas in human (V5) and macaque (STS; Kregelberg, Dannenberg, Hoffmann, Bremmer, & Ross, 2003; Kregelberg, Vatakis, & Kourtzi, 2005). The perception of motion in the pattern direction would occur because the form information enhances a motion representation in the consistent direction. The undirected motion energy, therefore, causes the greatest activation coincident with the pattern orientation.

## Summary

Our study shows that form information influences motion processing in a different manner than previously thought. Our results reveal that the orientation cues from motion streaks, which are detected in V1, influence motion direction processing at a later stage, most likely V5. We provide a new model of motion direction that gives a systematic explanation of how form information enters the motion system, which is unaccounted for by existing models of visual processing. This is important for understanding how the visual system recovers object motion, as it shows that form

information provides a strong constraint on motion processing.

*Keywords:* motion streaks, tDCS, form-motion interactions, motion modeling

## Acknowledgments

This work was supported by Australian Research Council grants DP130102580 and DP110104553 to DRB and DP120102313 to T. A. W. V. The University of Western Australia also provided a scholarship to M. F. T. We also thank Geoff Hammond for the access to the tDCS equipment.

Commercial relationships: none.

Corresponding author: Matthew F. Tang.

Email: matthew.tang@graduate.uwa.edu.au.

Address: School of Psychology, The University of Western Australia, Crawley, Western Australia, Australia.

## References

- Accornero, N., Li Voti, P., La Riccia, M., & Gregori, B. (2007). Visual evoked potentials modulation during direct current cortical polarization. *Experimental Brain Research*, *178*, 261–266. doi:10.1007/s00221-006-0733-y.
- Adelson, E. H., & Bergen, J. R. (1985). Spatiotemporal energy models for the perception of motion. *Journal of the Optical Society of America. A, Optics and Image Science*, *2*, 284–299. doi:10.1364/JOSAA.2.000284.
- Adelson, E. H., & Movshon, J. A. (1982). Phenomenal coherence of moving visual patterns. *Nature*, *300*, 523–525. doi:10.1038/300523a0.
- Albright, T. D. (1984). Direction and orientation selectivity of neurons in visual area MT of the macaque. *Journal of Neurophysiology*, *52*, 1106–1130.
- Amano, K., Edwards, M., Badcock, D. R., & Nishida, S. (2009a). Adaptive pooling of visual motion signals by the human visual system revealed with a novel multi-element stimulus. *Journal of Vision*, *9*(3):4, 1–25, doi:10.1167/9.3.4. [PubMed] [Article]
- Amano, K., Edwards, M., Badcock, D. R., & Nishida, S. (2009b). Spatial-frequency tuning in the pooling of one- and two-dimensional motion signals. *Vision Research*, *49*, 2862–2869. doi:10.1016/j.visres.2009.08.026.

- Antal, A., Kincses, T. Z., Nitsche, M. A., & Paulus, W. (2003). Manipulation of phosphene thresholds by transcranial direct current stimulation in man. *Experimental Brain Research*, *150*, 375–378. doi:10.1007/s00221-003-1459-8.
- Antal, A., Kovács, G., Chaieb, L., Cziraki, C., Paulus, W., & Greenlee, M. W. (2012). Cathodal stimulation of human MT+ leads to elevated fMRI signal: A tDCS-fMRI study. *Restorative Neurology and Neuroscience*, *30*, 255–263.
- Antal, A., Nitsche, M. A., Kincses, T. Z., Kruse, W., Hoffmann, K.-P., & Paulus, W. (2004). Facilitation of visuo-motor learning by transcranial direct current stimulation of the motor and extrastriate visual areas in humans. *European Journal of Neuroscience*, *19*, 2888–2892. doi:10.1111/j.1460-9568.2004.03367.x.
- Antal, A., Varga, E. T., Nitsche, M. A., Chadaide, Z., Paulus, W., Kovács, G., & Vidnyánszky, Z. (2004). Direct current stimulation over MT+/V5 modulates motion aftereffect in humans. *NeuroReport*, *15*, 2491–2494.
- Apthorp, D., & Alais, D. (2009). Tilt aftereffects and tilt illusions induced by fast translational motion: Evidence for motion streaks. *Journal of Vision*, *9*(1): 27, 1–11, doi:10.1167/9.1.27. [PubMed] [Article]
- Apthorp, D., Cass, J., & Alais, D. (2010). Orientation tuning of contrast masking caused by motion streaks. *Journal of Vision*, *10*(10):11, 1–13 doi:10.1167/10.10.11. [PubMed] [Article]
- Apthorp, D., Cass, J., & Alais, D. (2011). The spatial tuning of “motion streak” mechanisms revealed by masking and adaptation. *Journal of Vision*, *11*(7): 17, 1–16, doi:10.1167/11.7.17. [PubMed] [Article]
- Apthorp, D., Schwarzkopf, D. S., Kaul, C., Bahrami, B., Alais, D., & Rees, G. (2013). Direct evidence for encoding of motion streaks in human visual cortex. *Proceedings Biological Sciences*, *280*, 1–9. doi:10.1098/rspb.2012.2339.
- Apthorp, D., Wenderoth, P., & Alais, D. (2009). Motion streaks in fast motion rivalry cause orientation-selective suppression. *Journal of Vision*, *9*(5):10, 1–14, doi:10.1167/9.5.10. [PubMed] [Article]
- Badcock, D. R., & Dickinson, J. E. (2009). Second-order orientation cues to the axis of motion. *Vision Research*, *49*, 407–415. doi:10.1016/j.visres.2008.11.009.
- Badcock, D. R., McKendrick, A. M., & Ma-Wyatt, A. (2003). Pattern cues disambiguate perceived direction in simple moving stimuli. *Vision Research*, *43*, 2291–2301. doi:10.1016/S0042-6989(03)00403-6.
- Basole, A., White, L. E., & Fitzpatrick, D. (2003). Mapping multiple features in the population response of visual cortex. *Nature*, *423*, 986–990. doi:10.1038/nature01721.
- Beckers, G., & Zeki, S. (1995). The consequences of inactivating areas V1 and V5 on visual motion perception. *Brain*, *118*, 49–60. doi:10.1093/brain/118.1.49.
- Bex, P. J., & Dakin, S. C. (2002). Comparison of the spatial-frequency selectivity of local and global motion detectors. *Journal of the Optical Society of America. A, Optics, Image Science, and Vision*, *19*, 670–677.
- Blakemore, C., & Campbell, F. (1969). On the existence of neurones in the human visual system selectively sensitive to the orientation and size of retinal images. *Journal of Physiology*, *203*, 237–260.
- Born, R. T., & Bradley, D. C. (2005). Structure and function of visual area MT. *Annual Review of Neuroscience*, *28*, 157–189. doi:10.1146/annurev.neuro.26.041002.131052.
- Britten, K. H., & Newsome, W. T. (1998). Tuning bandwidths for near-threshold stimuli in area MT. *Journal of Neurophysiology*, *80*, 762–770.
- Burr, D. C., & Ross, J. (2002). Direct evidence that “speedlines” influence motion mechanisms. *Journal of Neuroscience*, *22*, 8661–8664.
- Carandini, M., & Ferster, D. (1997). A tonic hyperpolarization underlying contrast adaptation in cat visual cortex. *Science*, *276*, 949–952.
- Clifford, C. W. (2002). Perceptual adaptation: motion parallels orientation. *Trends in Cognitive Science*, *6*, 136–143.
- Clifford, C. W. (2014). The tilt illusion: Phenomenology and functional implications. *Vision Research*, *104*, 3–11. doi:10.1016/j.visres.2014.06.009.
- Clifford, C. W., Wenderoth, P., & Spehar, B. (2000). A functional angle on some after-effects in cortical vision. *Proceedings Biological Science*, *267*, 1705–1710.
- De Valois, K. K. (1977). Spatial frequency adaptation can enhance contrast sensitivity. *Vision Research*, *17*, 1057–1065. doi:10.1016/0042-6989(77)90010-4.
- De Valois, R. L., Albrecht, D. G., & Thorell, L. G. (1982). Spatial frequency selectivity of cells in macaque visual cortex. *Vision Research*, *22*, 545–559. doi:10.1016/0042-6989(82)90113-4.
- De Valois, R. L., William Yund, E., & Hepler, N. (1982). The orientation and direction selectivity of cells in macaque visual cortex. *Vision Research*, *22*(5), 531–544. doi:10.1016/0042-6989(82)90112-2.

- Dickinson, J. E., Almeida, R. A., Bell, J., & Badcock, D. R. (2010). Global shape aftereffects have a local substrate: A tilt aftereffect field. *Journal of Vision*, *10*(13):5, 1–12, doi:10.1167/10.13.5. [PubMed] [Article]
- Dickinson, J. E., & Badcock, D. R. (2013). On the hierarchical inheritance of aftereffects in the visual system. *Frontiers in Psychology*, *4*, 1–15. doi:10.3389/fpsyg.2013.00472.
- Dickinson, J. E., Harman, C., Tan, O., Almeida, R. A., & Badcock, D. R. (2012). Local contextual interactions can result in global shape misperception. *Journal of Vision*, *12*(11):3, 1–20, doi:10.1167/12.11.3. [PubMed] [Article]
- Dragoi, V., Sharma, J., & Sur, M. (2000). Adaptation-induced plasticity of orientation tuning in adult visual cortex. *Neuron*, *28*(1), 287–298.
- Edwards, M., & Badcock, D. R. (1994). Global motion perception: interaction of the ON and OFF pathways. *Vision Research*, *34*, 2849–2858. doi:10.1016/0042-6989(94)90054-X.
- Edwards, M., Cassanello, C. R., Badcock, D. R., & Nishida, S. (2013). Effect of form cues on 1D and 2D motion pooling. *Vision Research*, *76*, 94–104. doi:10.1016/j.visres.2012.10.015.
- Edwards, M., & Crane, M. F. (2007). Motion streaks improve motion detection. *Vision Research*, *47*, 828–833. doi:10.1016/j.visres.2006.12.005.
- Fang, F., Murray, S. O., Kersten, D., & He, S. (2005). Orientation-tuned fMRI adaptation in human visual cortex. *Journal of Neurophysiology*, *94*, 4188–4195.
- ffytche, D. H., Guy, C. N., & Zeki, S. (1996). Motion specific responses from a blind hemifield. *Brain*, *119*, 1971–1982. doi:10.1093/brain/119.6.1971.
- Geisler, W. S. (1999). Motion streaks provide a spatial code for motion direction. *Nature*, *400*, 65–69. doi:10.1038/21886.
- Geisler, W. S., Albrecht, D. G., Crane, A. M., & Stern, L. (2001). Motion direction signals in the primary visual cortex of cat and monkey. *Visual Neuroscience*, *18*, 501–516.
- Gibson, J. J., & Radner, M. (1937). Adaptation, aftereffect and contrast in the perception of tilted lines. I. Quantitative studies. *Journal of Experimental Psychology*, *20*, 453–467.
- Greenlee, M. W., & Magnussen, S. (1987). Saturation of the tilt aftereffect. *Vision Research*, *27*, 1041–1043. doi:10.1016/0042-6989(87)90017-4.
- Greenlee, M. W., & Magnussen, S. (1988). Interactions among spatial frequency and orientation channels adapted concurrently. *Vision Research*, *28*, 1303–1310.
- Heeger, D. J., Simoncelli, E. P., & Movshon, J. A. (1996). Computational models of cortical visual processing. *Proceedings of the National Academy of Sciences, USA*, *93*, 623–627.
- Homan, R. W., Herman, J., & Purdy, P. (1987). Cerebral location of international 10–20 system electrode placement. *Electroencephalography and Clinical Neurophysiology*, *66*, 376–382.
- Khuu, S. (2012). The role of motion streaks in the perception of the kinetic Zollner illusion. *Journal of Vision*, *12*(6):19, 1–14, doi:10.1167/12.6.19. [PubMed] [Article]
- Kohn, A., & Movshon, J. A. (2004). Adaptation changes the direction tuning of macaque MT neurons. *Nature Neuroscience*, *7*, 764–772. doi:10.1038/nn1267.
- Kooi, F. L. (1993). Local direction of edge motion causes and abolishes the barberpole illusion. *Vision Research*, *33*, 2347–2351. doi:10.1016/0042-6989(93)90112-A.
- Krekelberg, B., Dannenberg, S., Hoffmann, K.-P., Bremmer, F., & Ross, J. (2003). Neural correlates of implied motion. *Nature*, *424*, 674–677. doi:10.1038/nature01852.
- Krekelberg, B., Vatakis, A., & Kourtzi, Z. (2005). Implied motion from form in the human visual cortex. *Journal of Neurophysiology*, *94*, 4373–4386. doi:10.1152/jn.00690.2005.
- Kumano, H., & Uka, T. (2013). Responses to random dot motion reveal prevalence of pattern-motion selectivity in area MT. *Journal of Neuroscience*, *33*, 15161–15170. doi:10.1523/jneurosci.4279-12.2013.
- Lang, N., Nitsche, M. A., Paulus, W., Rothwell, J. C., & Lemon, R. N. (2004). Effects of transcranial direct current stimulation over the human motor cortex on corticospinal and transcallosal excitability. *Experimental Brain Research*, *156*, 439–443. doi:10.1007/s00221-003-1800-2.
- Levinson, E., & Sekuler, R. (1976). Adaptation alters perceived direction of motion. *Vision Research*, *16*, 779–781.
- Magnussen, S., & Johnsen, T. (1986). Temporal aspects of spatial adaptation. A study of the tilt aftereffect. *Vision Research*, *26*, 661–672. doi:10.1016/0042-6989(86)90014-3.
- McDonald, J. S., Seymour, K. J., Schira, M. M., Spehar, B., & Clifford, C. W. G. (2009). Orientation-specific contextual modulation of the fMRI BOLD response to luminance and chromatic

- gratings in human visual cortex. *Vision Research*, *49*, 1397–1405. doi:10.1016/j.visres.2008.12.014.
- Morrone, M. C., Burr, D. C., & Vaina, L. M. (1995). Two stages of visual processing for radial and circular motion. *Nature*, *376*, 507–509. doi:10.1038/376507a0.
- Motulsky, H., & Christopoulos, A. (2004). *Fitting models to biological data using linear and nonlinear regression: A practical guide to curve fitting*. Oxford, UK: Oxford University Press.
- Movshon, J. A., Adelson, E. H., Gizzi, M. S., & Newsome, W. T. (1985). The analysis of moving visual patterns. In C. Chagas, R. Gattass, & C. Gross (Eds.), *Pattern recognition mechanisms (Pontificiae Academiae Scientiarum Scripta Varia)* (Vol. 45. pp. 117–151). Rome: Vatican Press.
- Movshon, J. A., & Newsome, W. T. (1996). Visual response properties of striate cortical neurons projecting to area MT in macaque monkeys. *Journal of Neuroscience*, *16*, 7733–7741.
- Muir, D., & Over, R. (1970). Tilt aftereffects in central and peripheral vision. *Journal of Experimental Psychology*, *85*, 165–170. doi:10.1037/h0029509.
- Nitsche, M. A., Fricke, K., Henschke, U., Schlitterlau, A., Liebetanz, D., Lang, N., & Paulus, W. (2003). Pharmacological modulation of cortical excitability shifts induced by transcranial direct current stimulation in humans. *Journal of Physiology*, *553*(pt. 1), 293–301. doi:10.1113/jphysiol.2003.049916.
- Nitsche, M. A., & Paulus, W. (2000). Excitability changes induced in the human motor cortex by weak transcranial direct current stimulation. *Journal of Physiology*, *527*(pt. 3), 633–639.
- O'Toole, B., & Wenderoth, P. (1977). The tilt illusion: Repulsion and attraction effects in the oblique meridian. *Vision Research*, *17*, 367–374. doi:10.1016/0042-6989(77)90025-6.
- Robson, J. (1966). Spatial and temporal contrast sensitivity functions of the visual system. *Journal of the Optical Society of America. A, Optics, Image Science, and Vision*, *56*, 1141–1142.
- Rodman, H. R., & Albright, T. D. (1987). Coding of visual stimulus velocity in area MT of the macaque. *Vision Research*, *27*, 2035–2048. doi:10.1016/0042-6989(87)90118-0.
- Ross, J. (2004). The perceived direction and speed of global motion in Glass pattern sequences. *Vision Research*, *44*, 441–448. doi:10.1016/j.visres.2003.10.002.
- Ross, J., Badcock, D. R., & Hayes, A. (2000). Coherent global motion in the absence of coherent velocity signals. *Current Biology*, *10*, 679–682. doi:10.1016/S0960-9822(00)00524-8.
- Schrater, P. R., & Simoncelli, E. P. (1998). Local velocity representation: Evidence from motion adaptation. *Vision Research*, *38*, 3899–3912.
- Shadlen, M. N., Britten, K. H., Newsome, W. T., & Movshon, J. A. (1996). A computational analysis of the relationship between neuronal and behavioral responses to visual motion. *Journal of Neuroscience*, *16*, 1486–1510.
- Simoncelli, E. P., & Heeger, D. J. (1998). A model of neuronal responses in visual area MT. *Vision Research*, *38*, 743–761.
- Skillen, J., Whitaker, D., Popple, A. V., & McGraw, P. V. (2002). The importance of spatial scale in determining illusions of orientation. *Vision Research*, *42*, 2447–2455. doi:10.1016/S0042-6989(02)00261-4.
- Smith, A. T., Snowden, R. J., & Milne, A. B. (1994). Is global motion really based on spatial integration of local motion signals? *Vision Research*, *34*, 2425–2430. doi:10.1016/0042-6989(94)90286-0.
- Snowden, R. J., Treue, S., & Andersen, R. A. (1992). The response of neurons in areas V1 and MT of the alert rhesus monkey to moving random dot patterns. *Experimental Brain Research*, *88*, 389–400. doi:10.1007/BF02259114.
- Stagg, C. J., & Nitsche, M. A. (2011). Physiological basis of transcranial direct current stimulation. *Neuroscientist*, *17*, 37–53. doi:10.1177/1073858410386614.
- Tadini, L., El-Nazer, R., Brunoni, A. R., Williams, J., Carvas, M., Boggio, P., & Fregni, F. (2011). Cognitive, mood, and electroencephalographic effects of noninvasive cortical stimulation with weak electrical currents. *Journal of ECT*, *27*, 134–140. doi:10.1097/YCT.0b013e3181e631a8.
- Tang, M. F., Dickinson, J. E., Visser, T. A. W., Edwards, M., & Badcock, D. R. (2013). The shape of motion perception: Global pooling of transformational apparent motion. *Journal of Vision*, *13*(13):20, 1–2, doi:10.1167/13.13.20. [PubMed] [Article]
- Tootell, R. B. H., Hadjikhani, N. K., Vanduffel, W., Liu, A. K., Mendola, J. D., Sereno, M. I., & Dale, A. M. (1998). Functional analysis of primary visual cortex (V1) in humans. *Proceedings of the National Academy of Sciences, USA*, *95*, 811–817.
- Ware, C., & Mitchell, D. E. (1974). The spatial selectivity of the tilt aftereffect. *Vision Research*, *14*, 735–737. doi:10.1016/0042-6989(74)90072-8.
- Webb, B. S., Ledgeway, T., & McGraw, P. V. (2007).

Cortical pooling algorithms for judging global motion direction. *Proceedings of the National Academy of Sciences, USA*, 104, 3532–3537. doi:10.1073/pnas.0611288104.

Wenderoth, P., & Johnstone, S. (1988). The different mechanisms of the direct and indirect tilt illusions. *Vision Research*, 28, 301–312. doi:10.1016/0042-6989(88)90158-7.